JBC RESEARCH ARTICLE

Retinal-phospholipid Schiff-base conjugates and their interaction with ABCA4, the ABC transporter associated with Stargardt disease

Received for publication, December 8, 2022, and in revised form, March 10, 2023 Published, Papers in Press, March 16, 2023,
https://doi.org/10.1016/j.jbc.2023.104614

Tongzhou Xu, Laurie L. Molday, and Robert S. Molday*

From the Department of Biochemistry and Molecular Biology, University of British Columbia, Vancouver, Canada

Reviewed by members of the JBC Editorial Board. Edited by Kirill Martemyanov

***N*-retinylidene-phosphatidylethanolamine (*N*-Ret-PE), the Schiff-base conjugate formed through the reversible reaction of retinal (Vitamin A-aldehyde) and phosphatidylethanolamine, plays a crucial role in the visual cycle and visual pigment photoregeneration. However, *N*-Ret-PE can react with another molecule of retinal to form toxic di-retinoids if not removed from photoreceptors through its transport across photoreceptor membranes by the ATP-binding-cassette transporter ABCA4. Loss-of-function mutations in ABCA4 are known to cause Stargardt disease (STGD1), an inherited retinal degenerative disease associated with the accumulation of fluorescent di-retinoids and severe loss in vision. A larger assessment of retinal-phospholipid Schiff-base conjugates in photoreceptors is needed, along with further investigation of ABCA4 residues important for *N*-Ret-PE binding. In this study we show that *N*-Ret-PE formation is dependent on pH and phospholipid content. When retinal is added to liposomes or photoreceptor membranes, 40 to 60% is converted to *N*-Ret-PE at physiological pH. Phosphatidylserine and taurine also react with retinal to form *N*-retinylidene-phosphatidylserine and *N*-retinylidene-taurine, respectively, but at significantly lower levels. *N*-retinylidene-phosphatidylserine is not a substrate for ABCA4 and reacts poorly with retinal to form di-retinoids. Additionally, amino acid residues within the binding pocket of ABCA4 that contribute to its interaction with *N*-Ret-PE were identified and characterized using site-directed mutagenesis together with functional and binding assays. Substitution of arginine residues and hydrophobic residues with alanine or residues implicated in STGD1 significantly reduced or eliminated substrate-activated ATPase activity and substrate binding. Collectively, this study provides important insight into conditions which affect retinal-phospholipid Schiff-base formation and mechanisms underlying the pathogenesis of STGD1.**

Vertebrate vision is initiated when light converts the visual chromophore *11-cis* retinal to its *all-trans* isomer within the photoreceptor G-protein-coupled receptors, rhodopsin, and cone opsins. This results in a series of conformational transitions leading to the Meta II state of the visual pigment, activation of the visual cascade, decrease in intracellular cGMP level, closure of cyclic nucleotide-gated channels, and hyperpolarization of the photoreceptor cell in a process known as phototransduction (1, 2). Following photoexcitation, the Schiff-base linkage between retinal and opsin undergoes hydrolysis and all-*trans* retinal (ATR) is released into photoreceptor outer segment disc membranes where it is either reduced to all-*trans* retinol by retinol dehydrogenases such as RDH8 as part of the visual cycle (3, 4) or reacts reversibly with phosphatidylethanolamine (PE) to form the Schiff-base adduct, *N*-retinylidiene-phosphatidylethanolamine (*N*-Ret-PE) as illustrated in Figure 1*A*. *N*-Ret-PE plays a role in the photoregeneration of 11-*cis* retinal in blue light (5). However, *N*-Ret-PE is also a reactive compound and therefore has to be removed from photoreceptor outer segments to prevent photoreceptor degeneration and a loss in vision. ABCA4, a member of the ABC superfamily of membrane transporters localized within the rim region of rod and cone photoreceptor outer segment disc membranes (6, 7), facilitates the removal of retinoids from photoreceptors by flipping *N*-Ret-PE from the intradiscal to the cytoplasmic leaflet of disc membranes (8). ATR produced through the reversible dissociation of *N*-Ret-PE is then reduced to *all-trans* retinol by retinol dehydrogenases for the synthesis of *11-cis* retinal by the visual cycle and the regeneration of the visual pigment. ABCA4 also transports the *11-cis* isomer of *N*-Ret-PE in the same direction (9). This together with a chemical isomerization reaction clears *11-cis* retinal from disc membranes that is not required for the regeneration of visual pigments (10).

The importance of ABCA4 in the clearance of excess retinal from photoreceptors is highlighted by the finding that loss-of-function mutations in ABCA4 are known to cause Stargardt disease (STGD1), a relatively common macular degeneration characterized by the early loss in central vision, accumulation of fluorescent lipofuscin deposits, and progressive degeneration of photoreceptor and retinal pigment epithelial (RPE) cells (11–14). In the absence of ABCA4 transport activity, *N*-Ret-PE accumulates in disc membranes and reacts with another molecule of retinal to form the pyridinium di-retinoid compound A2-PE consisting of two molecules of retinal (vitamin A aldehyde) and one molecule of PE (15). Upon phagocytosis of photoreceptor outer segments, phosphatidic acid is removed

* For correspondence: Robert S. Molday, molday@mail.ubc.ca.

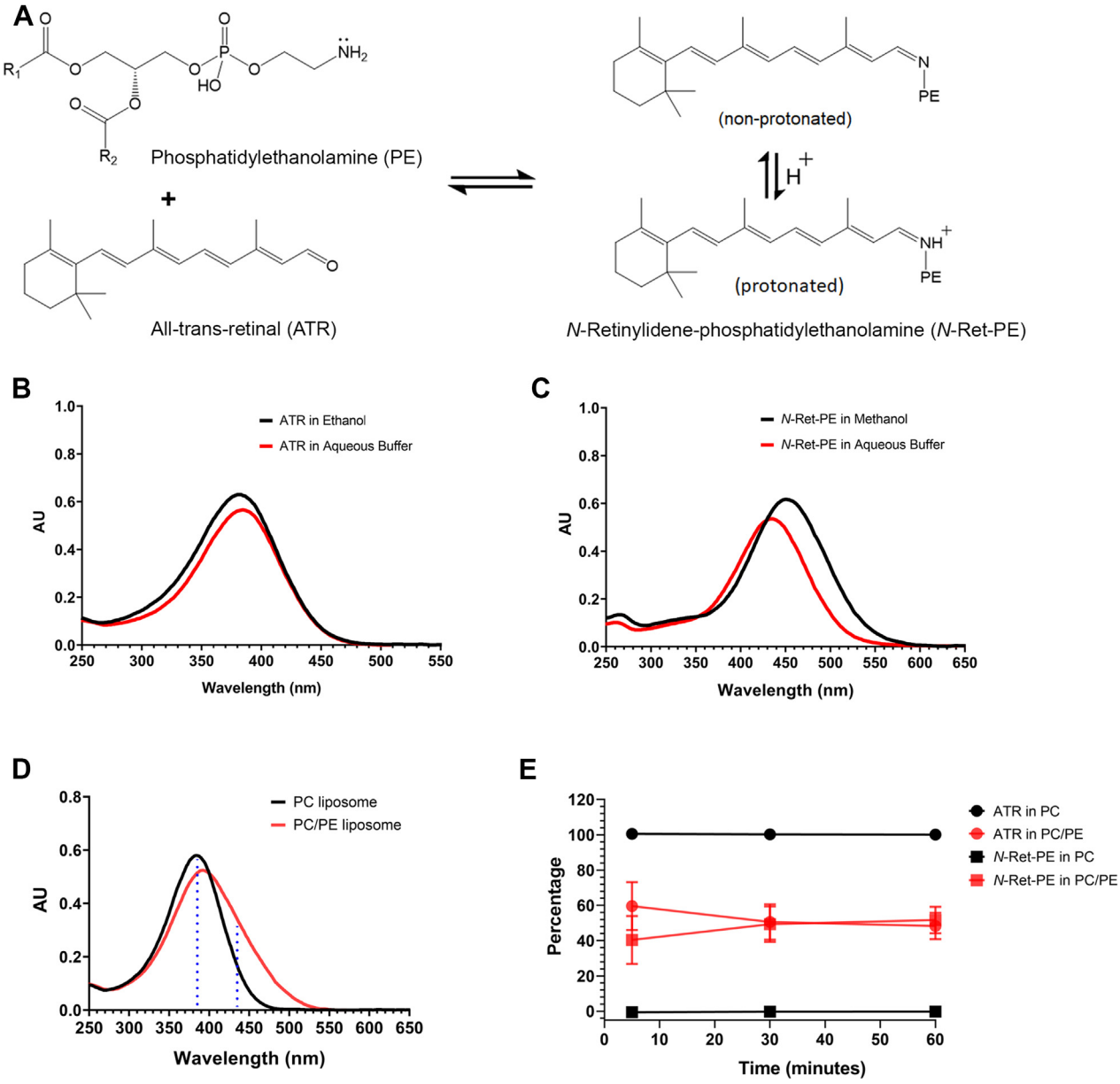

Figure 1. Spectral characterization of all-*trans* retinal and *N*-retinylidene-phosphatidylethanolamine (*N*-Ret-PE). *A*, reversible reaction of *all-trans* retinal (ATR) with phosphatidylethanolamine (PE) to form a mixture of nonprotonated and protonated *N*-Ret-PE. *B*, spectra of ATR in ethanol (λmax = 383 nm) and in aqueous buffer (acidified with TFA, 0.09 M Hepes Buffer pH 7.2, 0.9% CHAPS (w/v), 1.3% TFA (v/v)) (λmax = 385 nm). *C*, spectra of protonated *N*-Ret-PE in methanol acidified with 0.1% TFA (λmax = 450 nm) and in aqueous buffer (acidified with TFA) as above (λmax = 435 nm). *D*, representative spectra of ATR (20 μM) added to PC liposomes composed of 100% DOPC (57 μM) and PE/PC liposomes composed of 35% DOPE/65% DOPC (20 μM DOPE/37 μM DOPC) after 5 min. *Dotted blue lines* indicate wavelengths (385 nm and 435 nm) used to determine the percentages of ATR and *N*-Ret-PE at the endpoint. *E*, percentage of remaining ATR or *N*-Ret-PE formed over the sum of both determined after ATR was added to PC or PE/PC liposomes at 5 min, 30 min, or 60 min. Data represent mean ± S.D. (n = 3). CHAPS, 3-[(3-cholamidopropyl)dimethyl**a**mmonio]-1-propanesulfonate; DOPC, 1,2-dioleoyl-sn-glycero-3-phosphocholine; DOPE, 1,2-dioleoyl-sn-glycero-3-phosphoethanolamine; PC, phosphatidylcholine; TFA, trifluoroacetic acid.

from A2-PE by phospholipase D to produce A2-E in RPE cells where it accumulates with other di-retinoid compounds as fluorescent lipofuscin deposits leading to RPE and photoreceptor degeneration and a loss in vision (16–18). STGD1 affects as many as 1 in 6500 individuals and therefore is a prominent target for therapeutic intervention (10, 19–21).

The human *ABCA4* gene consisting of 50 exons encodes a 2273 amino acid membrane protein. This full-transporter is organized as two nonequivalent tandem halves, with each half containing a transmembrane domain (TMD) consisting of 6 membrane spanning segments, a nucleotide binding domain (NBD), and a large glycosylated exo-cytoplasmic domain (ECD) between the first and second membrane spanning segments of each TMD (22). Recently, the structures of ABCA4 in various states have been determined by cryo-EM (23–25). These studies have shown that the substrate-binding site is accessible through lateral diffusion of *N*-Ret-PE from the lumen leaflet of disc membranes. Binding of ATP to the NBDs results in a large conformational change converting substrate-bound ABCA4 from an open outward state

to a closed state. This coincides with the collapse of the substrate-binding site and the transport of *N*-Ret-PE to the cytoplasmic leaflet of the disc membrane. Hydrolysis of ATP within the NBDs resets ABCA4 to its open state allowing for the binding and transport of another molecule of *N*-Ret-PE.

Although considerable progress has been made in defining how retinoids are processed through the visual cycle and the identification of di-retinoids formed in the absence of ABCA4 transport activity, the extent to which ATR reacts with PE and other primary amine-containing compounds in photoreceptors to form their Schiff-base conjugates has not been systematically determined. Furthermore, our knowledge of key amino acid residues which are critical for the binding of *N*-Ret-PE to ABCA4 is incomplete.

In the present study we have used a spectrophotometric approach to quantify the extent to which ATR reacts with PE and other abundant primary amine-containing compounds to form their Schiff-base conjugates in liposomes and photoreceptor disc membranes under various conditions. In addition to PE, ATR was found to react with phosphatidylserine (PS) and taurine, to form their respective Schiff-base adducts but at significantly lower levels. *N*-retinylidene-phosphatidylserine (*N*-Ret-PS) formed through the reversible reaction of ATR and PS is not a substrate for ABCA4 and reacts poorly with ATR to form fluorescent di-retinoids. We have also identified key amino acid residues crucial for the binding of *N*-Ret-PE to ABCA4, several of which have been genetically linked to STGD1.

Results

Spectrophotometric analysis of ATR and N-*Ret-PE in liposomes*

ATR is known to react reversibly with the primary amine of PE to form the Schiff-base adduct, *N*-Ret-PE (Fig. 1*A*) (26, 27). The unprotonated form of *N*-Ret-PE has an UV-Visible spectrum with a λmax = 365 nm in methanol (5) which overlaps with that of ATR with a λmax = 383 nm in ethanol (28) and λmax 385 nm in acidified aqueous buffer (Fig. 1*B*). Under acidic conditions, the Schiff-base of *N*-Ret-PE is protonated (apparent pK 6.9 in liposomes (8)) resulting in a marked spectral red shift with a λmax = 450 nm in methanol and 435 nm in acidified aqueous buffer, for fully protonated *N*-Ret-PE (Fig. 1*C*). Accordingly, under physiological pH, free ATR is present together with protonated and unprotonated *N*-Ret-PE in PE-containing liposomal samples. This makes it difficult to directly measure the relative amounts of total *N*-Ret-PE and ATR in such preparations. To get around this problem, we rapidly added trifluoroacetic acid (TFA) to the liposomes to convert *N*-Ret-PE to its protonated form and to minimize the further formation of *N*-Ret-PE, while retaining ATR in its unmodified state.

In initial studies, 20 μM ATR was added to liposomes composed of 57 μM total phospholipid and containing either only 1,2-dioleoyl-sn-glycero-3-phosphocholine (DOPC) referred to as phosphatidylcholine (PC) liposomes or a molar mixture of 35% 1,2-dioleoyl-sn-glycero-3-phosphoethanolamine (DOPE) and 65% DOPC referred to as PE/PC liposomes to mimic the high PE content found in photoreceptor disc membranes (29). After incubation at room temperature (RT) for the indicated time, aliquots from the reaction mixtures were removed and quickly mixed with TFA to convert all *N*-Ret-PE to its protonated state and the spectrum was recorded after solubilization in 3-[(3-cholamidopropyl) dimethylammonio]-1-propanesulfonate (CHAPS) detergent. The amounts of total *N*-Ret-PE and ATR were determined from the absorbances at 385 nm and 435 nm (Fig. 1*D*) as described in detail in the Experimental Procedures.

When ATR was added to PC liposomes and incubated for 5 min, the UV-Visible spectrum still displayed a characteristic spectrum of ATR with a λmax of 385 nm (Fig. 1*D*). In contrast, the addition of ATR to PE/PC liposomes resulted in a significant spectral change within the first 5 min, indicating the formation of a significant fraction of *N*-Ret-PE (40% on average) and a corresponding decrease in ATR (Fig. 1, *D* and *E*). A further increase in *N*-Ret-PE to 49% of total retinoids occurred between 5 min and 30 min (Fig. *E*). A longer reaction time of 60 min resulted in no further statistically significant increase in *N*-Ret-PE (*t* test), indicating that equilibrium had been reached within the first 30 min.

Effect of PE concentration and pH on N-*Ret-PE formation*

Figure 2*A* shows the effect of adding 20 μM ATR to liposomes of varying phospholipid (PL) concentrations ranging from 14 to 228 μM and consisting of either 35% DOPE and 65% DOPC (PE/PC liposomes) or 100% DOPC (PC liposomes). A significant increase in the formation of *N*-Ret-PE was observed with increasing PL concentration for PE/PC liposomes. When the PL concentration was 14 μM (PE concentration of 5 μM = 1/4 the concentration of ATR), *N*-Ret-PE only accounted for 23% of total added retinoids for a 30 min time period (Fig. 2*A*). This increased to 64% when the PL concentration was increased to 228 μM (PE concentration of 80 μM, equaling 4 times the concentration of ATR). The increase in *N*-Ret-PE with increasing PL concentration is consistent with the increase in PE driving the equilibrium reaction toward the formation of *N*-Ret-PE. In contrast, no change in absorbance was observed when ATR was added to increasing concentrations of PC liposomes.

Next, we examined the effect of increasing the percentage of DOPE in PE/PC liposomes while maintaining the total PL and ATR concentration constant at 57 μM and 20 μM, respectively (Fig. 2*B*). As expected, a significant increase in *N*-Ret-PE formation occurred with increasing PE content. At 5% PE, *N*-Ret-PE formation was only 10% of the total retinoids, while at 45% PE, *N*-Ret-PE accounted for as much as 60% of the retinoids.

As part of this study, we also examined the effect of pH on the formation of *N*-Ret-PE in PE/PC liposomes for reaction times of 5 min and 30 min (Fig. 2*C*). For the shorter reaction time of 5 min, the fraction of *N*-Ret-PE at the end of the reaction increased from 22% at pH 5 to 71% at pH 9. For a 30 min reaction time, *N*-Ret-PE formation increased from 46% at pH 5 to 78% at pH 9. The increase in *N*-Ret-PE formation with increasing pH is consistent with an increase in the

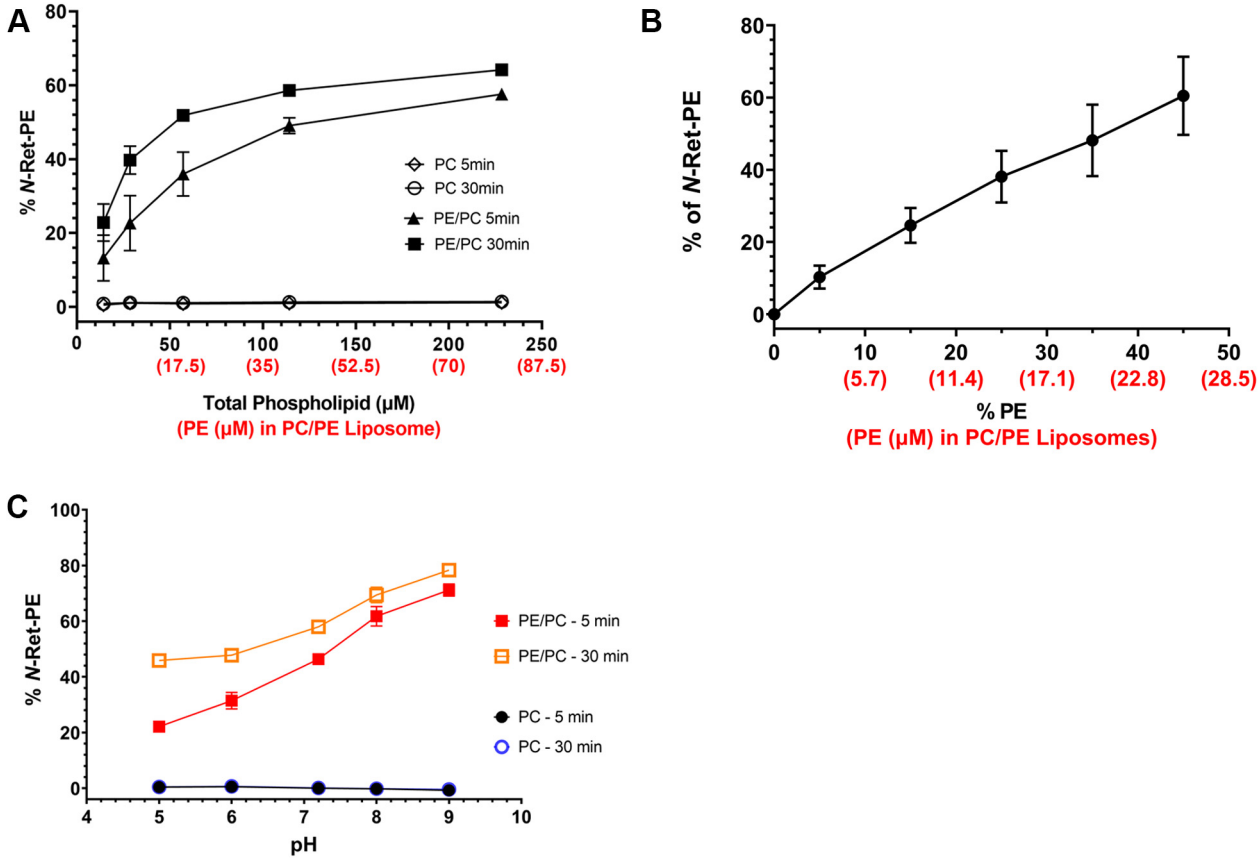

Figure 2. Effect of phospholipids and pH on the formation of *N*-Ret-PE. *A*, increase in *N*-Ret-PE as a function of increasing phospholipid concentration. ATR (20 μM) was added to PE/PC liposomes consisting of 35% DOPE and 65% DOPC or PC liposomes consisting of 100% DOPC with increasing total phospholipid concentrations for 5 min and 30 min. *B*, increase in *N*-Ret-PE with increasing PE content in PE/PC liposomes. ATR (20 μM) was added to liposomes containing increasing DOPE content and corresponding decrease in DOPC content while maintaining the total phospholipid concentration at 57 μM for a reaction time of 30 min. *C*, effect of pH on *N*-Ret-PE formation. ATR (20 μM) was added to 35% PE/65% PC liposomes (20 μM DOPE/37 μM DOPC) or 100% PC liposomes (57 μM DOPC) at various pH values. Data represent mean ± S.D. (n = 3 for panels A and C, and n = 4 for panel *B*). ATR, *all-trans* retinal; DOPC, 1,2-dioleoyl-sn-glycero-3-phosphocholine; DOPE, 1,2-dioleoyl-sn-glycero-3-phosphoethanolamine; *N*-Ret-PE, *N*-retinylidene-phosphatidylethanolamine; PC, phosphatidylcholine; PE, phosphatidylethanolamine.

unprotonated reactive form of PE at more basic pH which drives the initial reaction between the primary amine of PE and the aldehyde of ATR (apparent pK of PE = 9.6 (30)). The reduced level of *N*-Ret-PE produced at 5 min compared to 30 min reaction time, particularly evident at the lower pH, most likely reflects a slower formation of the Schiff-base at the shorter time due to the low concentration of unprotonated PE. In control reactions, no significant spectral change indicative of *N*-Ret-PE formation was evident over this pH range when ATR was added to PC liposomes for either reaction time.

Reaction of ATR with PS and taurine in liposomes

PS is another aminophospholipid present at relatively high concentrations (12% of the PL) in photoreceptor disc membranes (29). Figure 3*A* shows the spectral changes that occur when ATR is added to liposomes containing 12% 1,2-dioleoyl-sn-glycero-3-phosphoserine (DOPS) and 35% DOPS for comparison with liposomes containing the same percentages of DOPE. While the spectrum of liposome containing 12% DOPS was somewhat similar to that of ATR (Figs. 3*A* and 1*B*), a more noticeable shift was observed with 35% DOPS, indicative of the production of *N*-Ret-PS. However, the red-shifts of spectra in DOPS-containing liposomes relative to the spectrum of ATR were significantly smaller than those resulting from the reaction of ATR with PE in DOPE-containing liposomes at equivalent percentages.

Taurine is another primary amine-containing compound present at high concentrations in vertebrate retina (31). Previous studies have shown that *N*-retinylidene-taurine conjugates are present in the retina extracts as analyzed by HPLC although at very low levels (32, 33). To determine if ATR reacts with taurine in model PC liposomes, we measured the UV-Visible spectra of ATR in the presence and absence of 50 mM taurine. As shown in Figure 3*B*, an exceedingly small spectral change was observed upon the addition of ATR to PC liposomes in the presence of taurine.

The percentage of *N*-retinal-Schiff base conjugates formed in the presence of 20 μM ATR is compared for PS, PE, and taurine in Figure 3*C*. The amount of *N*-Ret-PS formed from the reaction of ATR and PS is lower than that for *N*-Ret-PE formation. At physiologically relevant PL contents (35% PE and 12%PS as found in photoreceptor disc membranes (29)), a 5.7-fold increase of *N*-Ret-PE compared with *N*-Ret-PS was

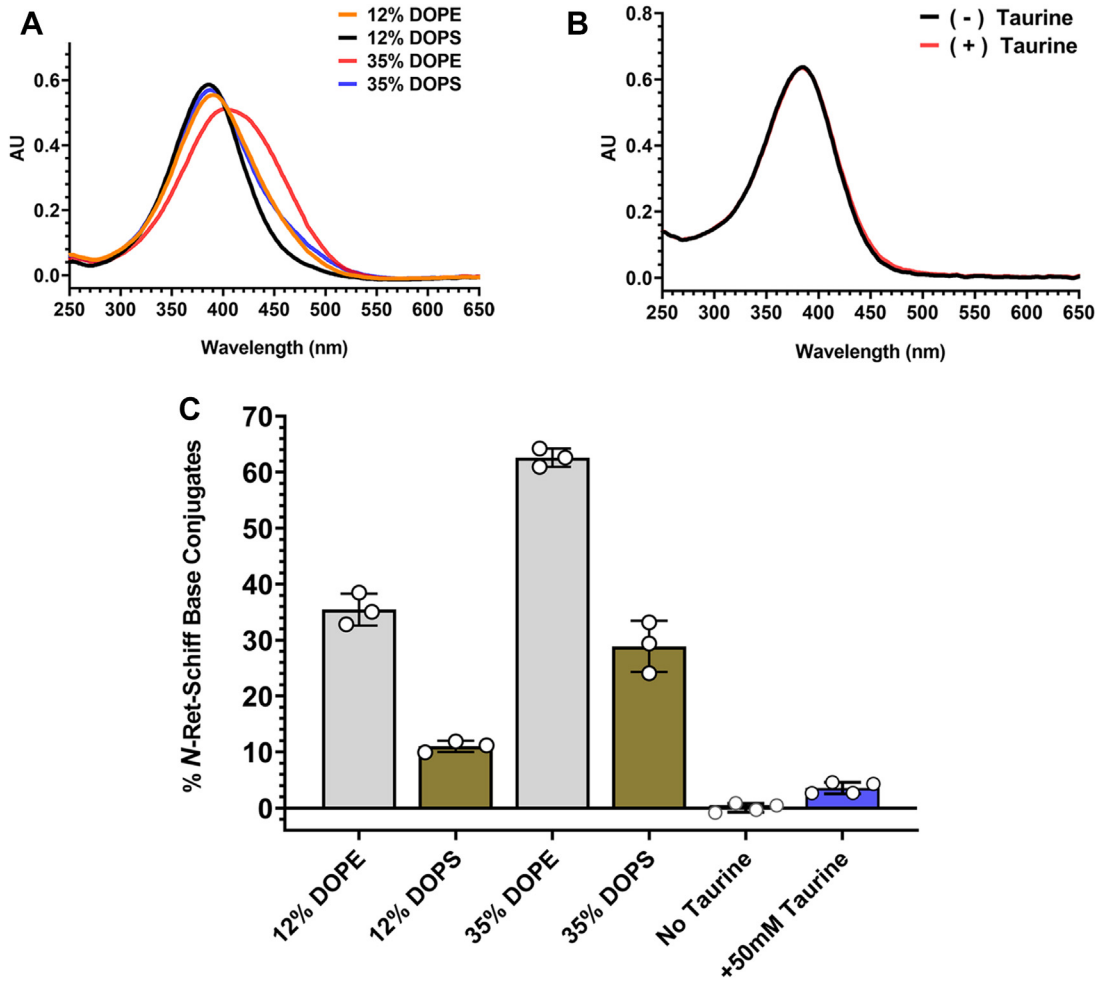

Figure 3. Characterization of *N*-Retinal-Schiff base conjugates. *A*, UV-Visible spectra of ATR/*N*-retinal-phospholipid-Schiff-base conjugate mixtures. ATR (20 μM) was added to liposomes consisting of 12% DOPE/88% DOPC, 12% DOPS/88% DOPC, 35% DOPE/65% DOPC, or 35% DOPS/65% DOPC (total phospholipid 228 μM) for 30 min. *B*, UV-Visible spectra of ATR/*N*-Retinal-Taurine Schiff-base conjugate mixture. ATR (20 μM) was added to PC liposomes composed of 100% DOPC (57 μM) with or without 50 mM taurine for 30 min. *C*, quantification of *N*-Ret-Schiff-base conjugates. The percentage of *N*-Ret-Schiff-base conjugates was quantified as described in the Experimental Procedures section. Data represent mean ± S.D. (n = 3 or 4 as indicated). ATR, *all-trans* retinal; DOPC, 1,2-dioleoyl-sn-glycero-3-phosphocholine; DOPE, 1,2-dioleoyl-sn-glycero-3-phosphoethanolamine; DOPS, 1,2-dioleoyl-sn-glycero-3-phosphoserine; PC, phosphatidylcholine.

observed in these model liposomes. Even when the amount of PS was increased to 35%, the amount of *N*-Ret-PS formed was significantly lower than the amount of *N*-Ret-PE formed at 35% PE. The Schiff-base conjugate formed through the reaction of ATR with 50 mM taurine was very low and marginally above control samples in the absence of taurine.

N-*retinylidene-phospholipids in photoreceptor membranes*

The formation of Schiff-base conjugates was measured in isolated bovine photoreceptor rod outer segment (ROS) membranes. For these studies, ROS membranes were illuminated with intense light in the presence of hydroxylamine (bleached) after determining the endogenous concentration of rhodopsin in the dark state (unbleached). Hydroxylamine reacts with ATR released after photoexcitation of rhodopsin to form the retinyloxime that is unreactive to PLs, thereby eliminating endogenous ATR in ROS. Exogeneous ATR equivalent to the amount of dark-state rhodopsin was subsequently added and the reaction was allowed to proceed for 5 and 30 min. The UV-Visible spectra were then recorded after the addition of TFA and CHAPS detergent. Figure 4*A* shows representative spectra of (1) unbleached, detergent-solubilized ROS membranes used to determine the concentration of rhodopsin; (2) bleached ROS (illuminated in the presence of hydroxylamine) followed by the addition of CHAPS and TFA; (3) bleached ROS supplemented with ATR and incubated at RT for 5 min; and (4) for 30 min (both with the addition of TFA and CHAPS). The spectra for the membranes treated with ATR for 5 and 30 min reflected the presence of external ATR and its Schiff-base conjugate(s), *N*-retinylidene-phospholipid (*N*-Ret-PL), which is most obvious in the difference spectra of the bleached ROS before and after the treatment of ATR (spectrum (3) or (4) minus spectrum (2), as shown in Figure 4*B*). From the different absorbances at 385 nm and 435 nm in the spectra of bleached ROS before and after the supplementation of exogenous ATR, we estimated that the ATR Schiff-base conjugate(s) formed, primarily

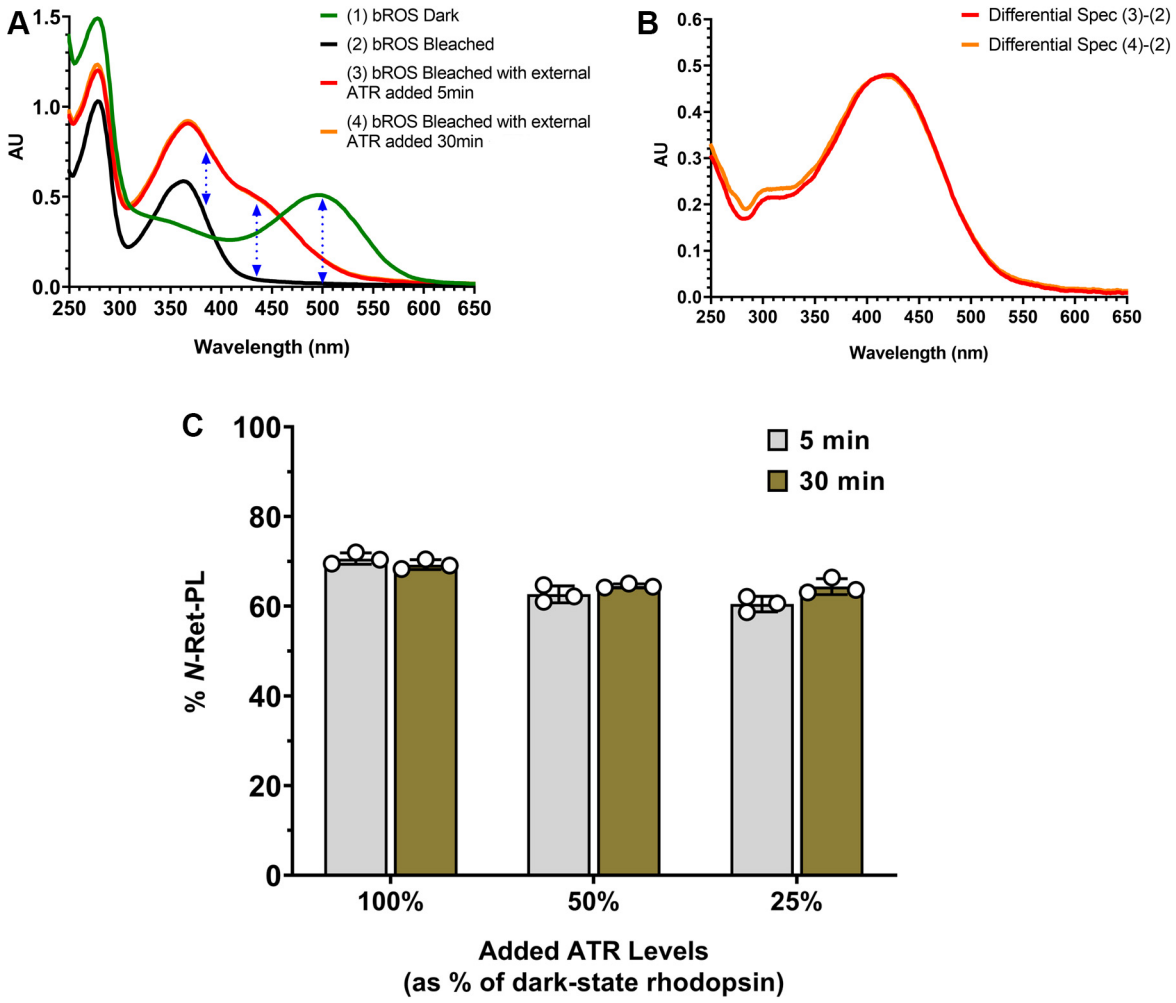

Figure 4. Formation and quantification of *N*-Ret-Phospholipid conjugates in rod outer segment (ROS) membranes. *A*, representative UV-Visible spectra: (1) Dark-state (unbleached) ROS membranes solubilized in detergent; (2) ROS membranes illuminated with intense light in the presence of hydroxylamine (bleached), followed by the addition of detergent and TFA; (3, 4) Bleached ROS membranes supplemented with external ATR equivalent to 100% of dark-state rhodopsin and incubated at RT for 5 min or 30 min respectively, followed by the addition of TFA and detergent. *Dotted blue lines* indicate the wavelengths used to determine the concentration of dark-state rhodopsin (500 nm) and the percentage of ATR and *N*-Ret-PL at the endpoint (385 nm and 435 nm). *B*, differential spectra between bleached ROS as indicated in (2) in panel *A* and bleached ROS after the addition of ATR as indicated in (3) or (4) in panel A. *C*, percentage of *N*-Ret-PL, primarily *N*-Ret-PE, formed in bleached ROS membranes supplemented with external ATR. ROS membranes illuminated in the presence of hydroxylamine were supplemented with external ATR equivalent to 100%, 50%, or 25% of the concentration of dark-state rhodopsin and the percentage of *N*-Ret-PL was determined after 5 min and 30 min reaction time. Data represent mean ± S.D. (n = 3). ATR, *all-trans* retinal; *N*-Ret-PE, *N*-retinylidene-phosphatidylethanolamine; *N*-Ret-PL, *N*-retinylidene-phospholipid; TFA, trifluoroacetic acid.

N-Ret-PE, accounted for 69 to 71% of the total external retinoids (ATR Schiff-base conjugate(s) and remaining ATR) at the indicated times (Fig. 4*C*) in the absence of reduction of ATR by retinol dehydrogenases (absence of NADPH cofactor). Similar percentages (61%–65%) were observed when the equivalent of 50% or 25% of ATR relative to the initial rhodopsin concentration was applied to bleached ROS membranes.

N-*Ret-PS is not a substrate for ABCA4*

Previously, we showed that the ATPase activity of ABCA4 is activated by *N*-Ret-PE when ATR is added to ABCA4 in the presence of PE (34, 35). This correlates with the transport of *N*-Ret-PE from the intradiscal to the cytoplasmic leaflet of disc membranes (8). Since ATR reacts with PS to form *N*-Ret-PS, we investigated if *N*-Ret-PS can also serve as a substrate for ABCA4. For these studies, we determined the ATPase activity of ABCA4 in the presence of PS with or without ATR using immunoaffinity-purified WT ABCA4. The ATPase activities of ABCA4 in the presence of PE (positive control) and PC (negative control) were measured in parallel. As shown in Figure 5*A*, the addition of ATR to detergent-solubilized ABCA4 in the presence of PE resulted in over a 2-fold increase in ATPase activity, as previously reported (34, 36). In contrast, ATR added to detergent-solubilized ABCA4 in the presence of PS or PC failed to stimulate the ATPase activity of ABCA4.

It is possible that *N*-Ret-PS binds to ABCA4 but does not activate its ATPase activity. To determine if *N*-Ret-PS stably interacts with ABCA4, we employed a radiolabeling assay previously used to confirm the binding of *N*-Ret-PE to ABCA4 in the absence of ATP and its release by the addition of nucleotide (37). In this assay, [^{3}H]-labeled ATR was added to ABCA4

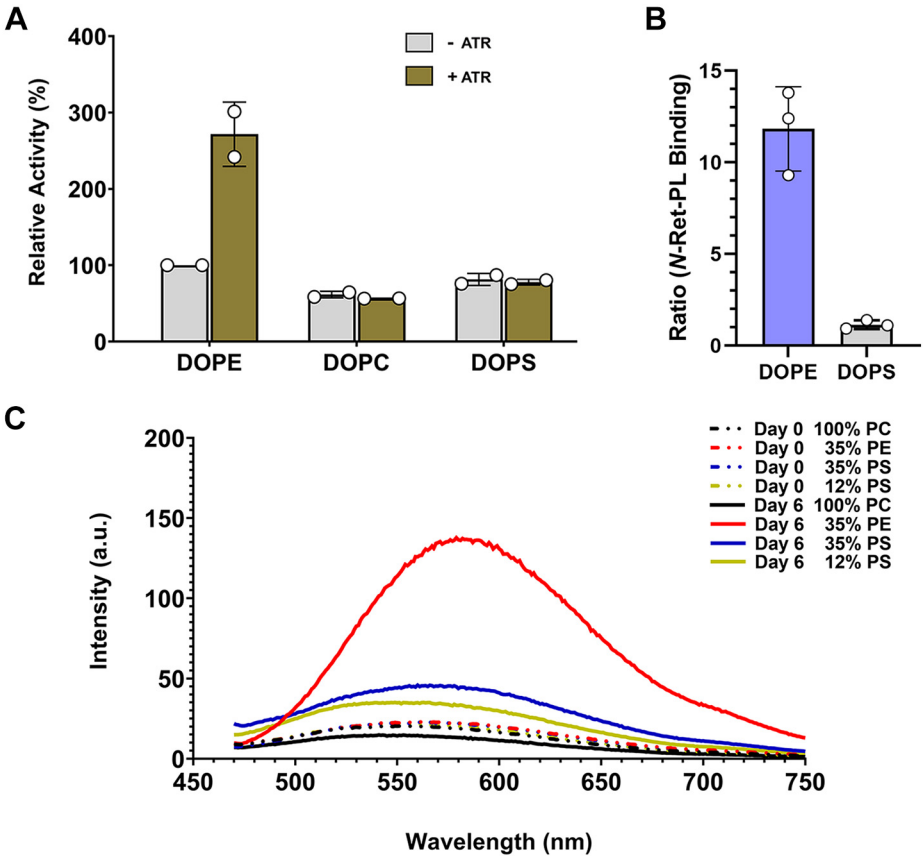

Figure 5. Interaction of *N*-Ret-PL conjugates with ABCA4 and fluorescence emission spectra from prolonged reaction of ATR in PC, PE/PC, or PS/PC liposomes. *A*, the ATPase activity of ABCA4 in the presence of DOPE, DOPS, or DOPC was measured in the absence (-ATR) and presence (+ATR) of 40 μM ATR used to generate *N*-Ret-PL conjugates. Data represent the mean ± S.D. for two independent experiments relative to the ATPase activity in the presence of DOPE and the absence of ATR. *B*, binding of N-Ret-PE or *N*-Ret-PS to ABCA4. Data displayed as a ratio of counts (dpm) for the binding of *N*-Ret-PE or *N*-Ret-PS in the absence of ATP to the binding in the presence of ATP for 3 independent experiments. *C*, representative fluorescence emission spectra from the reaction of ATR with liposomes composed of PE, PS, and PC. ATR (200 μM) was added to liposomes (228 μM total phospholipid) consisting of 100% DOPC, 35% DOPE/65% DOPC, 35% DOPS/65% DOPC, 12% DOPS/88% DOPC, and incubated at RT for 6 days. The fluorescence emission spectra were recorded 15 min after the addition of ATR on Day 0, and on Day 6. The excitation wavelength was set at 439 nm. Three spectra of each condition were recorded and a representative spectrum from each condition is shown. ATR, *all-trans* retinal; DOPC, 1,2-dioleoyl-sn-glycero-3-phosphocholine; DOPE, 1,2-dioleoyl-sn-glycero-3-phosphoethanolamine; DOPS, 1,2-dioleoyl-sn-glycero-3-phosphoserine; *N*-Ret-PL, *N*-retinylidene-phospholipid; PS, phosphatidylserine; PC, phosphatidylcholine; PE, phosphatidylethanolamine.

immobilized on an immunoaffinity matrix in a buffer containing PS to generate the Schiff-base conjugate or PE as a positive control. After a 30 min incubation, samples were further treated with or without 2 mM ATP. As shown in Figure 5*B*, there was no significant difference between the DOPS-treated samples in the presence or absence of ATP (the ratio of binding was close to 1). In contrast, significant binding of *N*-Ret-PE was observed for the DOPE-treated samples in the absence of ATP that was largely abolished by the addition of ATP, reflected by the high ratio of binding, as previously reported (37). Taken together, these studies indicate that *N*-Ret-PS, unlike *N*-Ret-PE, does not serve as a substrate for ABCA4.

ATR reacts with N-*Ret-PE and* N-*Ret-PS to form fluorescence compounds*

N-Ret-PE slowly reacts with the *trans* or *cis* isomers of retinal in photoreceptor membranes to produce the fluorescent compound A2-PE, the precursor of A2-E (9, 38, 16). A broad fluorescence emission spectrum with a λmax of ∼580 nm similar to that reported for A2-E (39) was obtained when 200 μM ATR was added to PE/PC liposomes containing 35% DOPE for 6 days at RT (Fig. 5*C*). In contrast, much weaker fluorescence intensity was produced when ATR was added to PS/PC liposomes containing 12% or 35% DOPS for the same time period. Only a minimal fluorescence signal presumably due to ATR and/or *N*-Ret-PL was observed on day 0 or when 100% PC liposomes was treated with ATR for 6 days.

Functional analysis of amino acid residues within the N-*Ret-PE–binding site of ABCA4*

Recent structural studies have shown that *N*-Ret-PE is wedged between TMD1, TMD2, and ECD1 of ABCA4 in its substrate-bound state (Fig. 6*A*) (23, 24). Two arginine residues (R653 and R587) form polar interactions with the negatively charged phosphate group of *N*-Ret-PE and the aromatic residues W339 and Y345 extending from ECD1 stabilize substrate binding *via* their interaction with the hydrophobic retinal group of *N*-Ret-PE (Fig. 6, *B* and *C*). In addition to these residues, two other aromatic residues (Y340 and F348) extending off the ECD1 and aliphatic residues, L1674, L1815,

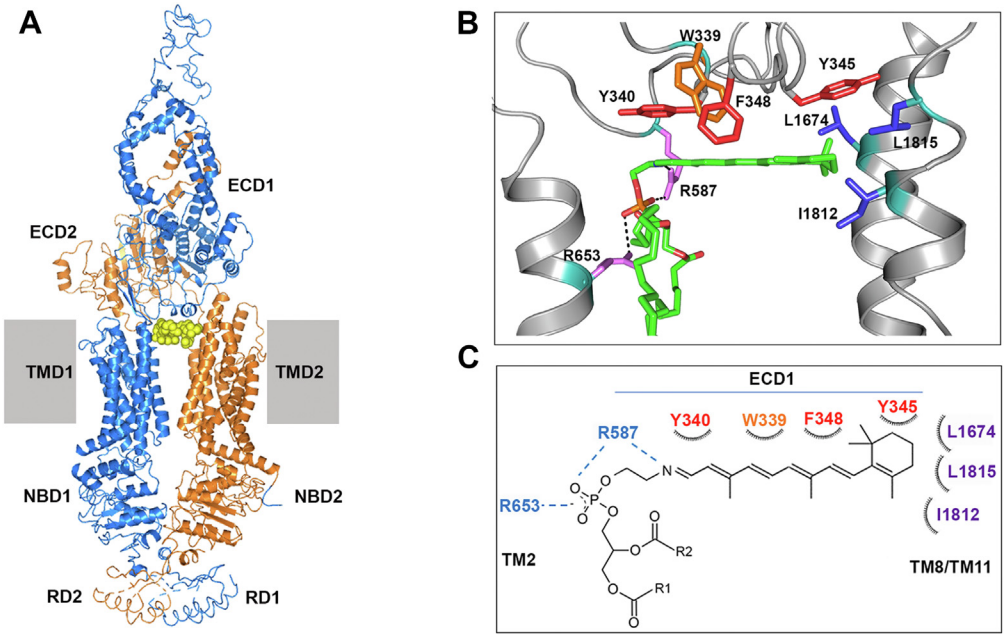

Figure 6. Schematic of the *N*-Ret-PE binding site of ABCA4. *A*, the structure of ABCA4 in its substrate-binding state showing ABCA4 as cartoon and bound *N*-Ret-PE as *yellow spheres*. The N-half of ABCA4 is shown in *marine blue* and the C-half in *orange*. *B*, *N*-Ret-PE binding site within the structure of ABCA4 in its substrate-bound state. Key polar, aromatic, and aliphatic side chains that come in close contact with *N*-Ret-PE are shown as sticks. *N*-Ret-PE substrate is shown as *green sticks*. *C*, schematic showing the binding site of *N*-Ret-PE; R1 and R2, fatty acyl chains; ECD, exo-cytoplasmic domain; *N*-Ret-PE, *N*-retinylidene-phosphatidylethanolamine; NBD, nucleotide-binding domain; RD, regulatory domai; TM, transmembrane segment; TMD, transmembrane domainn. (PDB 7M1P).

I1812 within transmembrane segments TM8 and TM11 also come in close contact with the retinoid group of *N*-Ret-PE. In order to determine the importance of these residues, we generated a series of mutants in which these residues were individually replaced with alanine or an amino acid implicated in STGD1. The effect of these variants on protein expression and basal and ATR-stimulated ATPase activities of ABCA4 and, in several cases, *N*-Ret-PE binding was investigated.

The expression profile of the ABCA4 variants is shown in representative western blots in Figure 7*A* and quantified in Figure 7*B*. All variants (Y340A, I1812A, L1815A, R587K, F348A, L1674A, Y340D) expressed at or close to WT levels, with the exception of the I1812N variant associated with STGD1 (40). This variant showed no detectable expression indicating that the protein was highly unstable.

The effect of these mutations on the basal and substrate-activated ATPase activity of ABCA4 was determined. For these studies, the variants were first isolated from HEK293T cell extracts by immunoaffinity chromatography and their purity confirmed on Coomassie blue stained SDS gels (Fig. 7*C*). The ATPase activity was then measured in the absence and presence of 40 μM ATR at similar protein concentrations. As shown in Figure 7*D*, the basal ATPase activity of all the variants was similar (70–100%) to that of WT ABCA4. Addition of ATR resulted in a 2-fold increase in activity for WT ABCA4 as previously reported (36, 41). The ATR-stimulated activity of the mutants varied, with the STGD1 mutants, Y340D and R587K, showing no significant substrate-activated activity. Although the activity of the alanine substitutions within the *N*-Ret-PE binding site (Y340A, F348A, L1674A, I1812A, L1815A) was activated by ATR, the ATR-activated activity in most cases was lower than that of WT ABCA4 (p-values for Y340A = 0.0110, F348A = 0.0844, L1674A = 0.0546, I1812A = 0.0396, L1815A = 0.0395, R587K = 0.0032, Y340D = 0.0086, two-tailed, paired t test, compared to the (+) ATR activity of WT ABCA4 in the corresponding experiments, n = 3).

To determine if the reduction in substrate-activated ATPase activity was due to the loss in substrate binding, we determined the extent to which *N*-Ret-PE bound to ABCA4 in the absence and presence of ATP. As previously shown, *N*-Ret-PE bound to ABCA4 in the absence of ATP. This binding was largely abolished in the presence of 2 mM ATP (Fig. 7*E*). Two ABCA4 variants, Y340D and R587K, showed no significant substrate binding in the absence or presence of ATP. The F348A variant, on the other hand, showed only a modest decrease in *N*-Ret-PE binding in the absence of ATP consistent with the substrate-activated ATPase activity measurements.

Discussion

Retinal, arguably the most important molecule in vision, is a highly reactive compound due to the potential of its aldehyde to react with primary amines to form Schiff-base conjugates. In photoreceptors, free retinal reversibly reacts with PE and other abundant primary amines, but the extent to which this occurs had not been previously studied, despite the fact that this information is crucial for understanding how retinal is processed as part of the visual system and the design and development of drug-based treatments for many retinal degenerative diseases including STGD1 (21, 42, 43).

In this study we quantified the level of Schiff-base conjugates formed through the reversible reaction of ATR with PE,

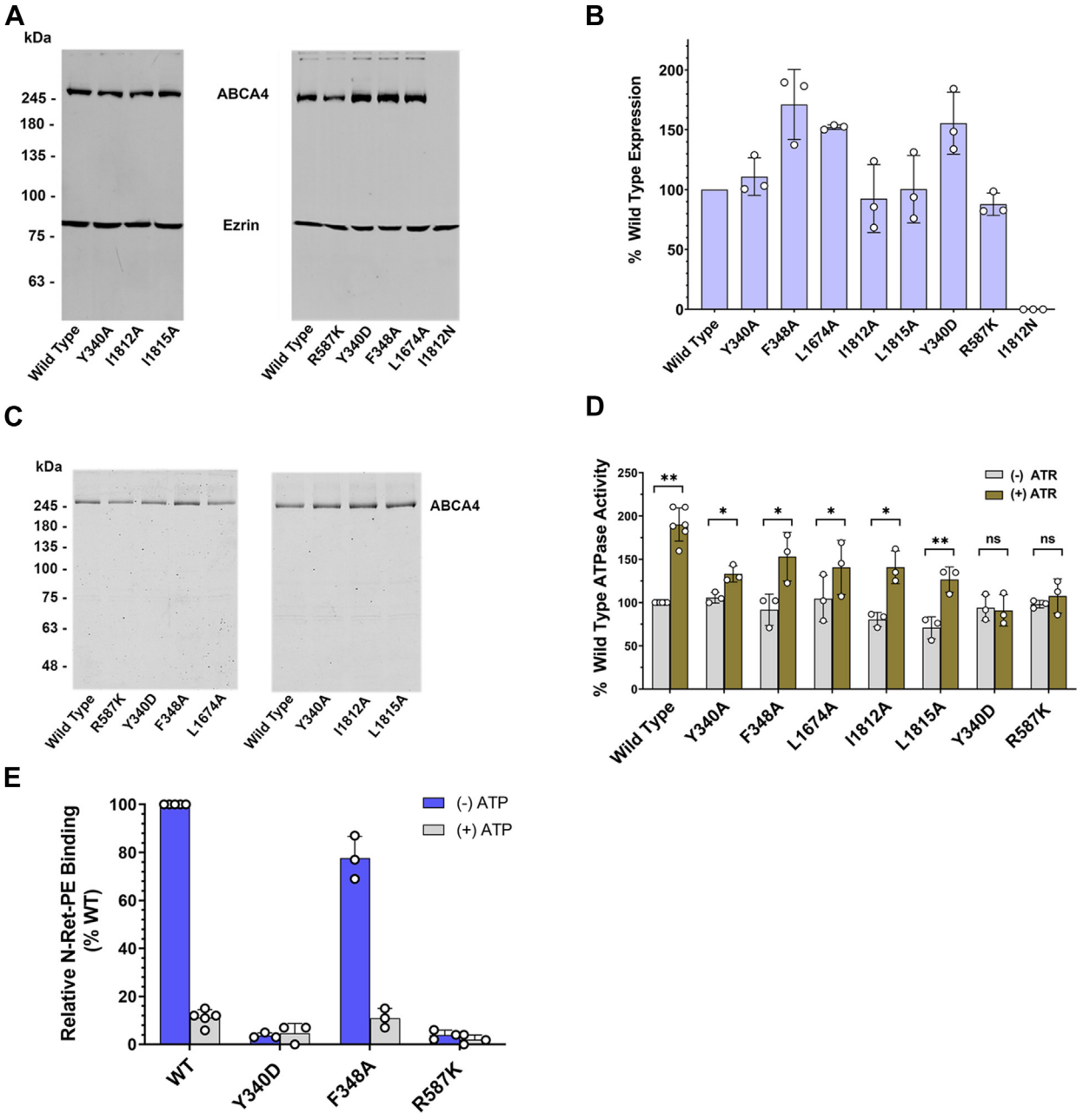

Figure 7. Analysis of amino acid substitutions within the *N*-Ret-PE binding site of ABCA4. *A*, representative Western blots showing the expression levels of ABCA4 variants. WT and mutant ABCA4 were expressed in HEK293T cells, solubilized in CHAPS detergent, and centrifuged to remove any non-solubilized material. The supernatant was applied to an SDS-polyacrylamide gel. Western blots were labeled with anti-Ezrin antibody (for loading control) and Rho 1D4 antibody (against the 9 amino acid 1D4 epitope tag engineered onto the C terminus of the ABCA4 proteins). *B*, quantification of the Western Blots for the expression of ABCA4 variants. The expression levels were normalized to that of WT ABCA4. Data represent Mean ± S.D. (n = 3 for each variant, n = 6 for WT). *C*, representative gel showing immunoaffinity purified WT and mutant ABCA4. The WT and mutant ABCA4 expressed in HEK293T cells were purified on Rho 1D4 immunoaffinity columns. Samples eluted with the 1D4 peptide were subjected to SDS gel electrophoresis and stained with Coomassie Blue. *D*, ATPase activity of affinity-purified WT and mutant ABCA4 in the absence and presence of 40 μM ATR normalized to the amount of purified protein. The activity was expressed relative to the basal activity (-ATR) of WT ABCA4 and presented as mean ± S.D. Two-tailed, paired *t* tests were carried out on the ATR-stimulated activity (+ATR) compared with the basal activity (-ATR) of the same protein for each ABCA4 mutant (n = 3) or WT (n = 6). The statistically significant difference is based on a *p*-value of < 0.05. *$p < 0.05$, **$p < 0.01$. (*p* values for WT=0.0001, Y340A = 0.0124, F348A = 0.0142, L1674A = 0.0145, I1812A = 0.0155, L1815A = 0.0010, Y340D = 0.3082, R587K = 0.4018) *E*, binding of *N*-Ret-PE to WT and ABCA4 variants in the absence and presence of 2 mM ATP. Data expressed as a mean ± SD. ATR, *all-trans* retinal; *N*-Ret-PE, *N*-retinylidene-phosphatidylethanolamine.

PS, and taurine in liposomes and photoreceptor outer segment disc membranes using a spectrophotometric approach. In model PE/PC liposomes, *N*-Ret-PE levels increased with increasing total PL concentration, PE content of the liposomes, and pH consistent with mass-action and the nucleophilic attack of the unprotonated form of PE on the aldehyde group of ATR as the first step in the formation of the Schiff-base conjugate. Under physiological conditions of pH, excess PL over ATR, and 35% PE content of the liposomes (Fig. 3*C*) over 60% of the total ATR was converted to *N*-Ret-PE. ATR also

reacts with PS in PS/PC liposomes but to a lesser degree. In liposomes consisting of 12% PS as found in photoreceptor outer segment disc membranes, only about 11% of the ATR was converted to *N*-Ret-PS (Fig. 3*C*). The combined reactions of ATR with physiological levels of PE and PS would result in ∼70% retinal-PL Schiff-base formation. This is comparable to the range of values (61%-71%) when various amounts of ATR (100%, 50%, and 25% the amount of rhodopsin) were added to photoreceptor disc membranes devoid of endogenous ATR and NADPH and ATP required for the activity of retinol dehydrogenases and ABCA4, respectively (Fig. 4). During preparation of this article for submission, Hong *et al.* (44), using a different approach, published a paper showing that as much as 40% of the free retinal added to ROS formed *N*-Ret-PE, in broad agreement with our studies.

The higher reactivity of ATR toward PE relative to PS is not only due to the higher content of PE in outer segment disc membranes but also to the lower pK value for the primary amine of PE than PS (30) resulting in a higher content of reactive unprotonated amine for the reaction of ATR with PE and possibly less steric hindrance. In contrast, ATR in PC liposome preparations minimally reacts with taurine even at 50 mM taurine concentration. This is likely due to the fact that taurine is a negatively-charged, polar molecule and accordingly is effectively excluded from the membrane bilayer where essentially all the ATR resides. The very low reactivity of taurine with retinal in membranes observed in our study is consistent with the low levels of the taurine Schiff-base conjugate detected in retinal extracts by HPLC (32).

A recent study has reported that *N*-Ret-PE can participate in the regeneration of visual pigments in both mammalian rods and cones by converting its all-*trans*-isomer to its 11-*cis* isomer under blue light (5). This supplements 11-*cis*-retinal in addition to the enzymatic visual cycle(s), specially in bright light when the high demand of visual pigments may not be fully satisfied by the visual cycle(s). That study also determined that in a dark-adapted mouse retina, *N*-Ret-PE accounts for ∼7% of total retinal pool (conjugated and nonconjugated) (5). Our study shows that when ATR is added to either PE-containing liposomes at physiological pH or photoreceptor outer segment membrane preparations, *N*-Ret-PE accounts for about half of total conjugated and nonconjugated retinal, indicating a significantly higher amount of *N*-Ret-PE will form in the light than in the dark. This finding reinforces the contribution of *N*-Ret-PE for the photoregeneration of 11-*cis*-retinal, especially under intense light condition, when the ATR yield from the photobleaching of visual pigment is very high and the formation of *N*-Ret-PE could increase accordingly.

Since *N*-Ret-PE itself is reactive, it together with *all-trans* and excess *11-cis* retinal has to be efficiently cleared from photoreceptor outer segments to prevent the production of toxic di-retinoids including A2-E that accumulate as fluorescent lipofuscin in the RPE cells of STGD1 patients and *Abca4* KO and transgenic mice (45–47). This is achieved through the ATP-dependent transport activity of ABCA4 that flips *N*-Ret-PE from the intradiscal to the cytoplasmic leaflet of disc membranes together with the reversible dissociation of *N*-Ret-PE into retinal and PE in the cytoplasmic leaflet of disc membranes (8, 9). Retinal can then be reduced to retinol for inclusion into the visual cycle(s) (3) and PE can redistribute across the disc membrane by the scramblase activity of the G-protein-coupled receptors, rhodopsin and cone opsins (48, 49) to maintain the symmetrical distribution of PE across the disc membrane (50). Although about 60% of ATR is converted to *N*-Ret-PE following a full-bleach of rod photoreceptors, about half likely resides in the intradiscal leaflet of disc membranes where it can serve as a substrate for ABCA4 since the PE is evenly distributed across disc membranes (50). Interestingly, although ATR can react with PS to form *N*-Ret-PS, this Schiff-base conjugate is not a substrate for ABCA4 (Fig. 5). A fraction of *N*-Ret-PS will be sequestered within the intradiscal leaflet of disc membranes. However, addition of ATR to liposomes containing 12% PS results in only a weak increase in fluorescence characteristic of di-retinoid compounds even when the PS content is increased to 35% of the PL. The low fluorescence signal produced when ATR is added to liposomes containing PS is primarily due to the lower amount of *N*-Ret-PS formed, but also may reflect a lower reactivity on *N*-Ret-PS with ATR, although this remains to be investigated. The low amount of *N*-Ret-PS and its limited reaction with ATR apparently does not necessitate a mechanism to transport *N*-Ret-PS across membranes. Instead, it can be cleared over time through the initial dissociation into retinal and PS within the intradiscal leaflet of photoreceptor membranes and the movement of retinal to the cytoplasmic leaflet by diffusion or through the formation of *N*-Ret-PE and its active transport by ABCA4.

N-Ret-PE is a highly amphipathic compound consisting of the negatively charged phosphate group and polar Schiff-base nitrogen flanked by the hydrophobic retinal moiety and the fatty acyl chains of variable length and unsaturation. Structural studies of ABCA4 in its substrate-bound state have shown that the negatively charged phosphate forms ionic bonds with the side chains of Arg653 (R653) from transmembrane segment 2 and Arg587 (R587) from ECD1 (23, 24). Arg587 also comes in close contact with the Schiff-base nitrogen of *N*-Ret-PE such that a hydrogen bond can further stabilize the interaction of nonprotonated *N*-Ret-PE with ABCA4 (Fig. 6, *B* and *C*). A previous study has shown that replacement of Arg653 with a lysine residue (R653K) retains substrate binding and substrate-activated ATPase activity of ABCA4, although the affinity of ABCA4 for its substrate is reduced by 2-fold (41). In the present study we examined the effect of replacing Arg587 with a lysine residue since this variant (R587K) has been implicated in STGD1 (51). The R587K variant displays a loss in substrate-activated ATPase activity without significantly affecting the expression or basal activity of ABCA4 as previously reported for the R587A variant (23). The loss in substrate-activated ATPase activity of the R587K variant correlates with the loss of substrate binding as shown in binding experiments (Fig. 7*E*). These results support genetic studies implicating this mutation in a severe form of STGD1. Several aromatic side chains extending from ECD1 come in close contact to the retinal moiety of *N*-Ret-PE. Previous studies showed that Trp339

(W339) and Tyr345 (Y345) residues are essential for the substrate binding and functional activity of ABCA4 (23, 24). We have extended this analysis to evaluate the role of two other aromatic (Tyr340 and Phe348) and aliphatic (Leu1674, Ile1812, and Leu1815) residues within the substrate-binding site on the activity of ABCA4. Substitution of these residues with alanine in most cases reduces but does not eliminate the substrate-stimulated ATPase activity. Substrate-stimulated activity and binding, however, are abolished for the Y340D variant supporting genetic studies implicating this variant in STGD1 (52). Evidently, an alanine substitution is sufficiently hydrophobic to reduce, but not abolish, substrate binding, whereas the negatively charged aspartic acid residue completely eliminates this interaction. The I1812N disease-associated variant is unusual in that the expression of this variant is undetectable in HEK293T cells. In this case, the replacement of the hydrophobic isoleucine residue with a highly polar asparagine residue likely causes global misfolding of the protein and rapid degradation by the quality control system of the cell. This is in contrast to the I1812A which shows WT-like expression and only a limited reduction in substrate-activated ATPase activity. Taken together, these results indicate that all the aromatic and aliphatic residues as well as the arginine residues within the substrate-binding site contribute to the high-affinity interaction of *N*-Ret-PE with ABCA4. Most disease-implicated ABCA4 variants harboring mutations in the substrate binding pocket including W339G, Y345C, R653C, Y340D, R587K, and I1812N are devoid of activity and hence are predicted to result in an early-onset, severe form of STGD1 (10).

In summary, our studies indicate that as much as 40 to 60% of retinal reacts with PE to form *N*-Ret-PE, about half of which is likely initially sequestered within the intradiscal leaflet of photoreceptor membranes where it can serve as a substrate for ABCA4. Retinal also reacts less efficiently with PS and taurine to form their Schiff-base conjugates. *N*-Ret-PS is not a substrate for ABCA4 and produces only a weak fluorescent signal characteristic of di-retinoids when incubated with ATR for 6 days. Therefore, its clearance through a transport mechanism is not required. Finally, *N*-Ret-PE interacts with ABCA4 through polar interactions with arginine side chains and nonpolar interactions with multiple aromatic and aliphatic side chains within the substrate-binding site. Disease-associated missense mutations in these residues cause a complete loss of substrate binding and function of ABCA4 either through a loss in protein expression as in the case of the I1812N variant or a loss in substrate-stimulated ATPase activity and substrate binding as shown in this study for the Y340D and R587K variants linked to STGD1. As a result, these mutations are predicted to cause an early onset and severe form of STGD1.

Experimental procedures

Materials

ATR was purchased from Sigma-Aldrich, Inc; DOPE, DOPS, DOPC, brain PC, and brain polar lipid (BPL) from Avanti Polar Lipids and CHAPS detergent from Anatrace. The Rho 1D4 antibody (53) was obtained from the University of British Columbia https://ubc.flintbox.com/technologies/0f1ef64b-fa5d-4a58-9003-3e01f6f672a6. The anti-Ezrin antibody (rabbit polyclonal) was purchased from Abcam (Cat. No. ab41672). The cDNA of human ABCA4 (NM_000350) containing a 1D4 tag (TETSQVAPA) at the C terminus has been described (54). Missense mutations were generated by PCR-based site-directed mutagenesis as described (55), using primers listed below. All DNA constructs were verified by Sanger sequencing.

Mutagenesis Primers:

ABCA4 I1812A.

Forward: 5′-CCTTCGCCTTGGAATTATTTGAGAATAACCGGACGC-3′

Reverse: 5′-CTCAAATAATTCCAAGGCGAAGGTAATAGCACTGC-3′

ABCA4 I1812N.

Forward: 5′-CCTTCAACTTGGAATTATTTGAGAATAACCGGACGC-3′

Reverse: 5′-CTCAAATAATTCCAAGTTGAAGGTAATAGCACTGC-3′

ABCA4 Y340A.

Forward: 5′-CAACTGGGCTGAAGACAATAACTATAAGGCC-3′

Reverse: 5′-GTTATTGTCTTCAGCCCAGTTGAAGGA-GAGC-3′

ABCA4 L1815A.

Forward: 5′-CTTGGAAGCATTTGAGAATAACCGGACGCTG-3′

Reverse: 5′-CCGGTTATTCTCAAATGCTTCCAAGATGAAGG-3′

ABCA4 F348A.

Forward: 5′-CTATAAGGCCGCTCTGGGGATTGACTCCACAAGG-3′

Reverse: 5′-CAATCCCCAGAGCGGCCTTATAGTTATTGTC-3′

ABCA4 L1674A.

Forward: 5′-GATTACAGTGGCGACCACTTCAGTGGATGC-3′

Reverse: 5′GTGGTCGCCACTGTAATCTCTGAGAGCTGCTC-3′

ABCA4 Y340D.

Forward: 5′-CAACTGGGATGAAGACAATAACTATAAGGCC-3′

Reverse: 5′- GTCTTCATCCCAGTTGAAGGAGAGCAC-3′

ABCA4 R587K.

Forward: 5′- GATTAAAGACAAGTATTGGGATTCTGGTCC-3′

Reverse: 5′- CCCAATACTTGTCTTTAATCTTATTGG-3′

Liposome preparations

Stock solutions of DOPC, DOPE, and DOPS in chloroform were stored at −30 °C under nitrogen gas. Liposomes were made by adding the desired molar percentage of PLs to glass tubes, drying down the PLs under a stream of nitrogen gas, and

subsequently resuspending the PLs in 0.1 M Hepes buffer, pH 7.2, except for studies in which the pH was varied. The resuspensions were vortexed vigorously for ~ 2 min, followed by stirring for ~ 15 min. The suspension was then sonicated with a probe-sonicator for ~ 15 s, followed by sonication in a bath sonicator for 35 min. In some cases, Hepes buffer was added to the liposomes to reach the targeted PL concentrations. The liposomes were used on the same day (in most cases) or stored at 4 °C for use the following day.

Formation and quantification of Schiff-base conjugates in liposomes

For analysis of *N*-Ret-PE levels, typically, a stock solution of 6 to 12 mM ATR in ethanol was added to liposomes (57 μM or indicated total PL concentration) consisting of 100% DOPC or DOPE/DOPC or DOPS/DOPC mixtures with the indicated molar percentage PLs under dim red light at RT to achieve a final concentration of 20 μM ATR. The solutions were vortexed and subsequently incubated in the dark at RT for the indicated times with intermittent mixing. At each time point, aliquots of 600 μl per condition were removed and added to glass tubes with 30 μl 30% (v/v) TFA. Subsequently, 60 μl of 10% CHAPS (w/v) was added with mixing and the UV-Visible spectrum was recorded using a DeNovix DS-11+ Spectrophotometer in a 10 mm cuvette. A solution of 600 μl 100% DOPC liposome (pH 7.2, without ATR) + 30 μl 30% TFA + 60 μl 10% CHAPS was used to adjust the baseline. The percentages of ATR and retinal-Schiff base conjugates at the endpoint were determined based on the absorbance at 385 nm and 435 nm as described below.

To estimate the percentage compositions of ATR or retinal-Schiff base conjugate in each condition, spectra of ATR in ethanol and aqueous buffer (0.09 M Hepes Buffer pH 7.2 : 0.9% CHAPS (w/v) and 1.3% TFA, made by mixing the same ratio of reagents for the final spectral measurement of the liposome samples) or *N*-Ret-PE in methanol acidified with 0.1% TFA and the same aqueous buffer were obtained (representative spectra shown in Fig. 1). The λmax of ATR = 383 nm in ethanol and 385 nm in the aqueous buffer. The λmax of protonated *N*-Ret-PE = 450 nm in methanol with 0.1% TFA and = 435 nm in the aqueous buffer. When the spectra of ATR of the same concentration were measured in both ethanol and the aqueous buffer, the molar extinction coefficient (ε) of ATR at 385 nm in the aqueous buffer can be calculated using the formula: $\varepsilon'_{(385nm,\ aqueous)} = AU_{(385nm,\ aqueous)} \times \varepsilon_{(383nm,\ ethanol)} / AU_{(383nm,\ ethanol)}$, where $\varepsilon_{(383nm,\ ethanol)}$ = 42,880 M^{-1} cm^{-1} (28). In our hands, the $\varepsilon'_{(385nm,\ aqueous)}$ of ATR = 38,389 M^{-1} cm^{-1} (calculated from the means of $AU_{(383nm,\ ethanol)}$ (n = 7) and $AU_{(385nm,\ aqueous)}$ (n = 7)). Similarly, the $\varepsilon'_{(435nm,\ aqueous)}$ of protonated *N*-Ret-PE =$AU_{(435nm,\ aqueous)} \times \varepsilon_{(450nm,\ methanol/TFA)} / AU_{(450nm,\ methanol/TFA)}$, where $\varepsilon_{(450nm,\ methanol/TFA)}$= 31,300 M^{-1} cm^{-1} (27). The $\varepsilon'_{(435nm,\ aqueous)}$ of protonated *N*-Ret-PE = 27,137 M^{-1} cm^{-1} (calculated from the means of $AU_{(450nm,\ methanol/TFA)}$ (n = 6) and $AU_{(435nm,\ aqueous)}$ (n = 7)). Moreover, in our aqueous buffer, the $AU_{(435nm)}/AU_{(385nm)}$ for ATR ≈ 0.2843 (mean from 7 spectra) and the $AU_{(385nm)}/AU_{(435nm)}$ for protonated *N*-Ret-PE ≈ 0.4907 (mean from 7 spectra). Assuming the absorbances of 385 nm and 435 nm in the final mixture were contributed by only ATR, or ATR and *N*-Ret-PE (or the other Schiff bases), the $AU_{(385nm)}$ from only ATR in the mixture was "a," and the $AU_{(435nm)}$ from only protonated *N*-Ret-PE (or the other Schiff bases) in the mixture was "b"

$a+0.4907b=AU_{(385nm/final)}$ of the final mixture.

$0.2843a+b=AU_{(435nm/final)}$ of the final mixture.

Therefore, the final concentrations of ATR and *N*-Ret-PE (or the other Schiff bases) could be estimated using the following equations:

$$a = \frac{AU(385nm/final) - 0.4907 \times AU(435nm/final)}{.0.8605}$$

$$b = \frac{AU(435nm/final) - 0.2843 \times AU(385nm/final)}{0.8605}$$

Thus, with the $\varepsilon'_{(385nm,\ aqueous)}$ of ATR (38,389 M^{-1} cm^{-1}) and the $\varepsilon'_{(435nm,\ aqueous)}$ of protonated *N*-Ret-PE (27,137 M^{-1} cm^{-1}), the percentage composition of ATR or its retinal-Schiff base conjugate at the endpoint could be estimated based on the concentrations of each over the sum of both, that is, ATR%= (a/38,389)/(a/38,389+b/27,137) x 100%, and *N*-Ret-PE (or the other Schiff- bases) %= (b/27,137)/(a/38,389+b/27,137) x 100%. Due to the similarity in the spectral characteristics of *N*-Ret-PE and *N*-Ret-PS (26), and the undetermined spectral characteristics of *N*-Ret-taurine, we used the same parameters of protonated *N*-Ret-PE for their estimation.

Formation and quantification of Schiff-base conjugates in bovine ROS

Bovine ROS were prepared from frozen-thawed bovine retinas (WL Lawson) in the dark as described (56). In each experiment, under dim red light, a sample of ROS was defrosted on ice and placed in a TLA110 centrifuge tube (Beckman Coulter, Canada). An aliquot of 2.6 to 3 ml of 0.1 M Hepes Buffer (pH 7.2) (referred to as Hepes Buffer hereafter) was added, mixed, and the suspension was centrifuged at ≥67,000g for 10 min at 4 °C. The supernatant was discarded and the pellet was resuspended with ~3.5 ml Hepes Buffer and centrifuged again. The second supernatant was discarded and the pellet was resuspended in Hepes Buffer of the same initial volume of ROS aliquot. An aliquot of 100 to 130 μl was removed and kept on ice in the dark for dark-state spectra measurement. The remaining resuspension was transferred to a 1.5 ml Eppendorf tube, with the addition of 30 μl of 1M hydroxylamine (pH 7.2) and Hepes Buffer to a final volume of 1.5 ml. The mixture was incubated at RT for ~40 min on a rolling rack standing above ice, illuminated with a 150W incandescent light bulb at a distance of about 10 to 15 cm. A translucent plastic panel was placed between the light bulb and

the rolling rack to reduce the heat and to diffuse the light. After bleaching, the mixture was transferred to a TLA 110 tube and the tube was filled up with Hepes Buffer (~2 ml) and centrifuged at 67,000g for 10 min at 4 °C. The pellet was washed four times by resuspending in 3.5 ml of Hepes Buffer and repeating the centrifugation. The final pellet was resuspended in Hepes Buffer of the same volume as the resuspension before the addition of hydroxylamine and bleaching.

Three to four aliquots of 30 μl each from the dark-state ROS (before bleach) saved previously were mixed with 270 μl Hepes Buffer and 30 μl 10% CHAPS to measure the dark-state spectra. The rhodopsin concentration in the dark state was then estimated based on the absorbances at 500 nm using the molar extinction coefficient of 40,600 M^{-1} cm^{-1} (57). Subsequently, four aliquots of 30 μl each from the bleached ROS were mixed with 270 μl Hepes Buffer, 30 μl 10% CHAPS, and 15 μl 10% TFA, to measure the "bleached" spectra. For the remaining bleached ROS, ATR in ethanol was added to final concentrations that matched the indicated percentages of concentrations of rhodopsin in the dark state. The mixtures were then incubated at RT in the dark, with intermittent mixing. At 5 min and 30 min time points, three aliquots of 30 μl each per condition were taken, and mixed with 270 μl Hepes Buffer and 15 μl 10% TFA that were preadded in glass tubes. Thirty μl of 10% CHAPS was added prior to recording the spectra. All the spectra were recorded using a DeNovix DS-11+ Spectrophotometer in a 10 mm cuvette, with the baseline set by a solution of 300 μl Hepes Buffer + 30 μl 10% CHAPS + 15 μl 10% TFA. The percentage of *N*-Ret-PL over the sum of itself and remaining ATR was estimated based on the AU_{385nm} and AU_{435nm} as described above, with the corresponding absorbances in the "bleached" spectra subtracted as the background.

Fluorescence measurements

PC liposomes consisting of 100% DOPC, PE/PC liposomes consisting of 35% DOPE/65% DOPC, and PS/PC liposomes consisting of either 12% DOPS/88% DOPC or 35% DOPS/65% DOPC (total lipid concentration of 228 μM) were treated with 200 μM ATR. After about 15 min at RT, the fluorescence emission spectra of aliquots of 200 μl each from these liposomes were recorded after solubilization with 20 μl 10% CHAPS (day 0). The 15-min incubation time was to allow the formation of most ATR-Schiff base conjugates, thus the fluorescence of which would be included as the background of the emission spectra on Day 0. Therefore, the increases of fluorescence from day 0 to day 6 would primarily reflect the formation of di-retinoids, which is known to be a slow reaction. The fluorescence emission spectrum of another aliquot of each sample was recorded when the reaction mixtures were maintained in the dark, with gently mixing at RT for 6 days (day 6). For fluorescent measurements, an excitation wavelength of 439 nm similar to the λmax for A2-E (38) was used and the emission spectra was recorded from 470 nm to 750 nm on a Varian Cary Eclipse Fluorescence Spectrophotometer. Three spectra of each condition were recorded and a representative spectrum from each condition was shown.

Expression, purification, and functional characterization of ABCA4 variants

The expression and purification of ABCA4 variants containing a 1D4 tag was carried out as described (55, 58). Briefly, HEK293T cells were transfected with plasmid DNA (5 μg per 10 cm plate or 1 μg per well of 6-well plate) using 1 mg/ml PEI MAX (Polysciences) at a 3:1 ratio of PEI to DNA. Cells were grown in a humidified incubator (5% CO_2) at 37 °C in Dulbecco's modified Eagle's medium supplemented with 8% bovine growth serum. Typically, cells were harvested ~ 24 h posttransfection and either used the same day (in most cases) or snap-frozen in liquid nitrogen and stored at −70 °C.

For the ABCA4 variant expression test, cells were transfected in 6-well plates and the cells from each well was resuspended in 25 μl of Buffer A (25 mM Hepes, pH 7.4, 150 mM NaCl, 5 mM $MgCl_2$, 10% glycerol, 1 mM DTT) with protease inhibitor cocktail (PIC) (Calbiochem 539,134) and solubilized by adding the resuspension slowly to 125 μl of a buffer of Buffer A with 24 mM CHAPS, PIC, and Benzonase nuclease (1:10,000) with stirring for 30 min at 4 °C.

For ABCA4 functional tests, cells were transfected in 10 cm plates. The harvested cells were resuspended in 100 μl per 10 cm plate of Buffer A with PIC and solubilized by adding the resuspension slowly to 0.5 ml per plate of Buffer A supplemented with 0.15 mg/ml BPL, 0.05 mg/ml DOPE, with 24 mM CHAPS and PIC with stirring, and kept stirring for 30 min at 4 °C. Typically, 2 to 3 plates of cells per ABCA4 variant were pooled in each experiment.

The solubilized cells for either test was then centrifuged at 67,000 to 72,000*g* for 12 min at 4 °C to remove nonsolubilized material, the supernatants were either subjected to SDS-gel electrophoresis and Western blotting to measure expression levels or mixed with 80 to 90 μl of Rho1D4-Sepharose 2B affinity matrix per ABCA4 variant for 1 h at 4 °C for purification (for the functional tests). In the latter case, the affinity matrix was washed nine times in Buffer A containing 0.15 mg/ml BPL, 0.05 mg/ml DOPE, and10 mM CHAPS. The protein was eluted two times with 56 to 66 μl each in the same buffer with 0.3 mg/ml 1D4 peptide at 18 °C for 30 min per time with mixing. A fraction was analyzed on SDS gels stained with Coomassie blue to determine the protein concentration using bovine serum albumin as a standard.

In the experiments designed to measure the effect of PE, PC, and PS individually on the activity of WT ABCA4, ~0.19 g pellets of suspension HEK 293T cells expressing WT ABCA4-1D4 was resuspended in 570 μl Buffer A with PIC, and solubilized by adding it slowly to 2.28 ml Buffer A with 0.1 mg/ml brain PC, 25 mM CHAPS and PIC with stirring for 30 min at 4 °C. After centrifugation, the supernatants were incubated with 240 μl of the Rho1D4 matrix for 1 h at 4 °C with mixing. The mixture was then divided equally into three aliquots (for

testing three types of lipids), washed three times in Buffer A containing 10 mM CHAPS and 0.1 mg/ml brain PC, followed by washing six times in Buffer A containing 10 mM CHAPS and 0.1 mg/ml of the corresponding lipid (DOPE/DOPC/DOPS). The aliquots were then eluted two times with 70 µl of 0.5 mg/ml 1D4 peptide in the respective buffer for each type of lipid at 18 °C for 30 min per time with mixing.

The functional activity of the purified WT ABCA4 and ABCA4 variants was measured as described using the ADP-Glo Kinase Assay protocol (Promega). Briefly, a 20 µl ATPase reaction was performed by incubating 15 µl of protein elution (typically containing ∼100–240 ng protein for the cells on plate or ∼440–720 ng protein for the suspension cells) with either 1 µl of 0.8 mM ATR or buffer for 15 min followed by the addition of 4 µl of 2.5 mM ultrapure ATP. The reaction was carried out for 35 min at 37 °C. Each reaction was done in triplicate. Five µl of each reaction was then mixed with 5 µl of ADP-Glo reagent in a well of a 384 Corning white polystyrene plate and incubated at RT for 1 h. Ten µl of kinase detection reagent was then added and the reaction mixture was incubated at RT for ∼35 min. The luminescence signal was detected using SoftMax Pro 5.4 on a Molecular Device SpectraMax M3 Spectrometer (https://www.moleculardevices.com/products/microplate-readers/acquisition-and-analysis-software/softmax-pro-software). Background control was carried out under the same conditions except for the addition of the ADP-Glo reagent at zero time (immediately following the addition of ATP). The luminescence signals after background subtraction were normalized to the purified protein amounts used in the assay and presented relative to the level of WT ABCA4 in the absence of ATR. Three independent experiments were carried out for each ABCA4 variant unless otherwise indicated and the data were expressed as the mean ± S.D.

N-*Ret-PE and N-Ret-PS binding studies*

The binding of *N*-Ret-PE to ABCA4 in the presence of DOPE or DOPS was carried out as described (55). Briefly, HEK293T cells expressing ABCA4-1D4 were solubilized in Buffer A containing 18 mM CHAPS, 0.01 mg/ml DOPC and PIC, and incubated for 20 min at RT with 20 µM of tritiated ATR (500 dpm/pmol). For each PL, the sample was divided into two aliquots. One was further incubated in Buffer A containing 10 mM CHAPS and 0.1 mg/ml DOPE or DOPS and the other was incubated in the same buffer but containing 2 mM ATP. After 30 min, the samples were applied to a Rho1D4 affinity column, washed six times with their respective buffer, and the bound tritiated retinoid was extracted in ethanol for measurement of radioactivity by liquid scintillation counting and the column subsequently treated with SDS to extract protein for Western blotting as described (55). The binding of tritiated ATR to ABCA4 variants was carried out as above with the following modification as described (41). HEK293T cells expressing the ABCA4 variants were solubilized in 18 mM CHAPS buffer containing 0.19 mg/ml BPL and 0.033 mg/ml DOPE prior to immobilization on a Rho1D4-Sepharose matrix and extraction as described above.

Statistical analysis

Statistics were carried out using GraphPad Prism 9.0 (https://www.graphpad.com/features). n-values are for number of independent experiments. *p*-values are as indicated in the text and legends.

Data availability

Additional data that support the findings of this study are available from the corresponding author upon reasonable request.

Author contributions—T. X. and L. L. M. methodology; T. X. and L. L. M. investigation; T. X., L. L. M., and R. S. M. visualization; T. X. and L. L. M. validation; T. X. and L. L. M. writing–reviewing and editing; R. S. M. writing–original draft preparation; T. X., L. L. M., and R. S. M. formal analysis; R. S. M. conceptualization.

Funding and additional information—This work was supported by grants from the Canadian Institutes of Health Research (CIHR): PJT 148649 and PJT 175118 to R. S. M.

Conflict of interest—The authors declare that they have no conflicts of interest with the contents of this article.

Abbreviations—The abbreviations used are: ATR, all-trans retinal; BPL, brain polar lipid; CHAPS, 3-[(3-cholamidopropyl)dimethylammonio]-1-propanesulfonate; DOPC, 1,2-dioleoyl-sn-glycero-3-phosphocholine; DOPE, 1,2-dioleoyl-sn-glycero-3-phospho ethanolamine; DOPS, 1,2-dioleoyl-sn-glycero-3-phosphoserine; ECD, exo-cytoplasmic domain; NBD, nucleotide binding domain; *N*-Ret-PE, *N*-retinylidene-phosphatidylethanolamine; *N*-Ret-PL, N-retinylidene-phospholipid; *N*-Ret-PS, *N*-retinylidene-phosphatidylserine; PC, phosphatidylcholine; PE, phosphatidylethanolamine; PIC, protease inhibitor cocktail; PL, phospholipid; PS, phosphatidylserine; ROS, rod outer segment; RPE, retinal pigment epithelial; RT, room temperature; STGD1, Stargardt disease; TFA, trifluoroacetic acid; TMD, transmembrane domain.

References

1. Luo, D. G., Xue, T., and Yau, K. W. (2008) How vision begins: an odyssey. *Proc. Natl. Acad. Sci. U. S. A.* **105**, 9855–9862
2. Hofmann, K. P., and Lamb, T. D. (2022) Rhodopsin, light-sensor of vision. *Prog. Retin. Eye Res.* **93**, 101116
3. Saari, J. C. (2012) Vitamin A metabolism in rod and cone visual cycles. *Annu. Rev. Nutr.* **32**, 125–145
4. Kiser, P. D., Golczak, M., and Palczewski, K. (2014) Chemistry of the retinoid (visual) cycle. *Chem. Rev.* **114**, 194–232
5. Kaylor, J. J., Xu, T., Ingram, N. T., Tsan, A., Hakobyan, H., Fain, G. L., *et al.* (2017) Blue light regenerates functional visual pigments in mammals through a retinyl-phospholipid intermediate. *Nat. Commun.* **8**, 16
6. Illing, M., Molday, L. L., and Molday, R. S. (1997) The 220-kDa rim protein of retinal rod outer segments is a member of the ABC transporter superfamily. *J. Biol. Chem.* **272**, 10303–10310
7. Molday, Rabin, A. R., and Molday, R. S. (2000) ABCR expression in foveal cone photoreceptors and its role in Stargardt macular dystrophy. *Nat. Genet.* **25**, 257–258

8. Quazi, F., Lenevich, S., and Molday, R. S. (2012) ABCA4 is an N-retinylidene-phosphatidylethanolamine and phosphatidylethanolamine importer. *Nat. Commun.* **3**, 925
9. Quazi, F., and Molday, R. S. (2014) ATP-binding cassette transporter ABCA4 and chemical isomerization protect photoreceptor cells from the toxic accumulation of excess 11-cis-retinal. *Proc. Natl. Acad. Sci. U. S. A.* **111**, 5024–5029
10. Molday, R. S., Garces, F. A., Scortecci, J. F., and Molday, L. L. (2022) Structure and function of ABCA4 and its role in the visual cycle and Stargardt macular degeneration. *Prog. Retin. Eye Res.* **89**, 101036
11. Allikmets, R., Singh, N., Sun, H., Shroyer, N. F., Hutchinson, A., Chidambaram, A., *et al.* (1997) A photoreceptor cell-specific ATP-binding transporter gene (ABCR) is mutated in recessive Stargardt macular dystrophy. *Nat. Genet.* **15**, 236–246
12. Tanna, P., Strauss, R. W., Fujinami, K., and Michaelides, M. (2017) Stargardt disease: clinical features, molecular genetics, animal models and therapeutic options. *Br. J. Ophthalmol.* **101**, 25–30
13. Cremers, F. P. M., Lee, W., Collin, R. W. J., and Allikmets, R. (2020) Clinical spectrum, genetic complexity and therapeutic approaches for retinal disease caused by ABCA4 mutations. *Prog. Retin. Eye Res.* **79**, 100861
14. Boyer, N. P., Higbee, D., Currin, M. B., Blakeley, L. R., Chen, C., Ablonczy, Z., *et al.* (2012) Lipofuscin and N-retinylidene-N-retinylethanolamine (A2E) accumulate in retinal pigment epithelium in absence of light exposure: their origin is 11-cis-retinal. *J. Biol. Chem.* **287**, 22276–22286
15. Sakai, N., Decatur, J., Nakanishi, K., and Eldred, G. E. (1996) Ocular age pigment "A2-E": an unprecedented pyridinium bisretinoid. *J. Am. Chem. Soc.* **118**, 1559–1560
16. Sparrow, J. R., Gregory-Roberts, E., Yamamoto, K., Blonska, A., Ghosh, S. K., Ueda, K., *et al.* (2012) The bisretinoids of retinal pigment epithelium. *Prog. Retin. Eye Res.* **31**, 121–135
17. Kim, H. J., and Sparrow, J. R. (2021) Bisretinoid phospholipid and vitamin A aldehyde: shining a light. *J. Lipid Res.* **62**, 100042
18. Liu, J. H., Itagaki, Y., Ben-Shabat, S., Nakanishi, K., and Sparrow, J. R. (2000) The biosynthesis of A2E, a fluorophore of aging retina, involves the formation of the precursor, A2-PE, in the photoreceptor outer segment membrane. *J. Biol. Chem.* **275**, 29354–29360
19. Hanany, M., Rivolta, C., and Sharon, D. (2020) Worldwide carrier frequency and genetic prevalence of autosomal recessive inherited retinal diseases. *Proc. Natl. Acad. Sci. U. S. A.* **117**, 2710–2716
20. Piotter, E., McClements, M. E., and MacLaren, R. E. (2021) Therapy approaches for Stargardt disease. *Biomolecules* **11**, 1179
21. Huang, D., Heath Jeffery, R. C., Aung-Htut, M. T., McLenachan, S., Fletcher, S., Wilton, S. D., *et al.* (2021) Stargardt disease and progress in therapeutic strategies. *Ophthalmic Genet.* **43**, 1–26
22. Bungert, S., Molday, L. L., and Molday, R. S. (2001) Membrane topology of the ATP binding cassette transporter ABCR and its relationship to ABC1 and related ABCA transporters: identification of N-linked glycosylation sites. *J. Biol. Chem.* **276**, 23539–23546
23. Scortecci, J. F., Molday, L. L., Curtis, S. B., Garces, F. A., Panwar, P., Van Petegem, F., *et al.* (2021) Cryo-EM structures of the ABCA4 importer reveal mechanisms underlying substrate binding and Stargardt disease. *Nat. Commun.* **12**, 5902
24. Xie, T., Zhang, Z., Fang, Q., Du, B., and Gong, X. (2021) Structural basis of substrate recognition and translocation by human ABCA4. *Nat. Commun.* **12**, 3853
25. Liu, F., Lee, J., and Chen, J. (2021) Molecular structures of the eukaryotic retinal importer ABCA4. *Elife* **10**, e63524
26. Plack, P. A., and Pritchard, D. J. (1969) Schiff bases formed from retinal and phosphatidylethanolamine, phosphatidylserine, ethanolamine or serine. *Biochem. J.* **115**, 927–934
27. Anderson, R. E., and Maude, M. B. (1970) Phospholipids of bovine outer segments. *Biochemistry* **9**, 3624–3628
28. Barua, A. B., Olson, J. A., Furr, H. C., and Van Breemen, R. B. (2000) *Vitamin A and Carotenoids in Modern Chromatographic Analysis of Vitamins*. In: De Leenheer, L.,W. E., Van Bocxlaer, J. F., eds. MARCEL DEKKER, INC, New York: 1–68
29. Fliesler, S. J., and Anderson, R. E. (1983) Chemistry and metabolism of lipids in the vertebrate retina. *Prog. Lipid Res.* **22**, 79–131
30. Tsui, F. C., Ojcius, D. M., and Hubbell, W. L. (1986) The intrinsic pKa values for phosphatidylserine and phosphatidylethanolamine in phosphatidylcholine host bilayers. *Biophys. J.* **49**, 459–468
31. Orr, H. T., Cohen, A. I., and Carter, J. A. (1976) The levels of free taurine, glutamate, glycine and gamma-amino butyric acid during the postnatal development of the normal and dystrophic retina of the mouse. *Exp. Eye Res.* **23**, 377–384
32. Kim, H. J., Zhao, J., and Sparrow, J. R. (2020) Vitamin A aldehyde-taurine adduct and the visual cycle. *Proc. Natl. Acad. Sci. U. S. A.* **117**, 24867–24875
33. Petrosian, A. M., Haroutounian, J. E., Gundersen, T. E., Blomhoff, R., Fugelli, K., and Kanli, H. (2000) New HPLC evidence on endogenous tauret in retina and pigment epithelium. *Adv. Exp. Med. Biol.* **483**, 453–460
34. Sun, H., Molday, R. S., and Nathans, J. (1999) Retinal stimulates ATP hydrolysis by purified and reconstituted ABCR, the photoreceptor-specific ATP-binding cassette transporter responsible for Stargardt disease. *J. Biol. Chem.* **274**, 8269–8281
35. Ahn, J., Wong, J. T., and Molday, R. S. (2000) The effect of lipid environment and retinoids on the ATPase activity of ABCR, the photoreceptor ABC transporter responsible for Stargardt macular dystrophy. *J. Biol. Chem.* **275**, 20399–20405
36. Curtis, S. B., Molday, L. L., Garces, F. A., and Molday, R. S. (2020) Functional analysis and classification of homozygous and hypomorphic ABCA4 variants associated with Stargardt macular degeneration. *Hum. Mutat.* **41**, 1944–1956
37. Beharry, S., Zhong, M., and Molday, R. S. (2004) N-retinylidene-phosphatidylethanolamine is the preferred retinoid substrate for the photoreceptor-specific ABC transporter ABCA4 (ABCR). *J. Biol. Chem.* **279**, 53972–53979
38. Parish, C. A., Hashimoto, M., Nakanishi, K., Dillon, J., and Sparrow, J. (1998) Isolation and one-step preparation of A2E and iso-A2E, fluorophores from human retinal pigment epithelium. *Proc. Natl. Acad. Sci. U. S. A.* **95**, 14609–14613
39. Sparrow, J. R., Parish, C. A., Hashimoto, M., and Nakanishi, K. (1999) A2E, a lipofuscin fluorophore, in human retinal pigmented epithelial cells in culture. *Invest. Ophthalmol. Vis. Sci.* **40**, 2988–2995
40. Sung, Y.-C., Yang, C.-H., Yang, C.-M., Lin, C.-W., Huang, D.-S., Huang, Y.-S., *et al.* (2020) Genotypes predispose phenotypes—clinical features and genetic spectrum of ABCA4-associated retinal dystrophies. *Genes* **11**, 1421
41. Garces, F. A., Scortecci, J. F., and Molday, R. S. (2021) Functional characterization of ABCA4 missense variants linked to Stargardt macular degeneration. *Int. J. Mol. Sci.* **22**, 185
42. Travis, G. H., Golczak, M., Moise, A. R., and Palczewski, K. (2007) Diseases caused by defects in the visual cycle: retinoids as potential therapeutic agents. *Annu. Rev. Pharmacol. Toxicol.* **47**, 469–512
43. Kiser, P. D., and Palczewski, K. (2016) Retinoids and retinal diseases. *Annu. Rev. Vis. Sci.* **2**, 197–234
44. Hong, J. D., Salom, D., Kochman, M. A., Kubas, A., Kiser, P. D., and Palczewski, K. (2022) Chromophore hydrolysis and release from photoactivated rhodopsin in native membranes. *Proc. Natl. Acad. Sci. U. S. A.* **119**, e2213911119
45. Mata, N. L., Weng, J., and Travis, G. H. (2000) Biosynthesis of a major lipofuscin fluorophore in mice and humans with ABCR-mediated retinal and macular degeneration. *Proc. Natl. Acad. Sci. U. S. A.* **97**, 7154–7159
46. Zhang, N., Tsybovsky, Y., Kolesnikov, A. V., Rozanowska, M., Swider, M., Schwartz, S. B., *et al.* (2015) Protein misfolding and the pathogenesis of ABCA4-associated retinal degenerations. *Hum. Mol. Genet.* **24**, 3220–3237
47. Molday, L. L., Wahl, D., Sarunic, M. V., and Molday, R. S. (2018) Localization and functional characterization of the p.Asn965Ser (N965S) ABCA4 variant in mice reveal pathogenic mechanisms underlying Stargardt macular degeneration. *Hum. Mol. Genet.* **27**, 295–306
48. Menon, I., Huber, T., Sanyal, S., Banerjee, S., Barre, P., Canis, S., *et al.* (2011) Opsin is a phospholipid flippase. *Curr. Biol.* **21**, 149–153

49. Ernst, O. P., and Menon, A. K. (2015) Phospholipid scrambling by rhodopsin. *Photochem. Photobiol. Sci.* **14**, 1922–1931
50. Hessel, E., Herrmann, A., Muller, P., Schnetkamp, P. P., and Hofmann, K. P. (2000) The transbilayer distribution of phospholipids in disc membranes is a dynamic equilibrium evidence for rapid flip and flop movement. *Eur. J. Biochem.* **267**, 1473–1483
51. Hu, F. Y., Li, J. K., Gao, F. J., Qi, Y. H., Xu, P., Zhang, Y. J., *et al.* (2019) ABCA4 gene screening in a Chinese cohort with Stargardt disease: identification of 37 novel variants. *Front. Genet.* **10**, 773
52. Shroyer, N. F., Lewis, R. A., and Lupski, J. R. (2000) Complex inheritance of ABCR mutations in Stargardt disease: linkage disequilibrium, complex alleles, and pseudodominance. *Hum. Genet.* **106**, 244–248
53. Hodges, R. S., Heaton, R. J., Parker, J. M., Molday, L., and Molday, R. S. (1988) Antigen-antibody interaction. Synthetic peptides define linear antigenic determinants recognized by monoclonal antibodies directed to the cytoplasmic carboxyl terminus of rhodopsin. *J. Biol. Chem.* **263**, 11768–11775
54. Zhong, M., and Molday, R. S. (2010) Binding of retinoids to ABCA4, the photoreceptor ABC transporter associated with Stargardt macular degeneration. *Methods Mol. Biol.* **652**, 163–176
55. Garces, F., Jiang, K., Molday, L. L., Stohr, H., Weber, B. H., Lyons, C. J., *et al.* (2018) Correlating the expression and functional activity of ABCA4 disease variants with the phenotype of patients with Stargardt disease. *Invest. Ophthalmol. Vis. Sci.* **59**, 2305–2315
56. Molday, R. S., and Molday, L. L. (1987) Differences in the protein composition of bovine retinal rod outer segment disk and plasma membranes isolated by a ricin-gold-dextran density perturbation method. *J. Cell Biol.* **105**, 2589–2601
57. Wald, G., and Brown, P. K. (1953) The molar extinction of rhodopsin. *J. Gen. Physiol.* **37**, 189–200
58. Zhong, M., Molday, L. L., and Molday, R. S. (2009) Role of the C terminus of the photoreceptor ABCA4 transporter in protein folding, function, and retinal degenerative diseases. *J. Biol. Chem.* **284**, 3640–3649